Structure development by reaction-induced phase separation in polymer mixtures: computer simulation of the spinodal decomposition under the non-isoquench depth

Takashi Ohnaga*, Wenjie Chen† and Takashi Inoue‡
Department of Organic and Polymeric Materials, Tokyo Institute of Technology, Ookayama, Meguro-ku, Tokyo 152, Japan
(Received 10 November 1993; revised 12 January 1994)

It has been shown that, in various thermoset/thermoplastic and monomer/polymer mixtures, demixing is induced by polymerization and it proceeds via the spinodal decomposition (SD) to yield the regularly phase-separated morphology. However, the SD is expected to take place under successive increases in quench depth. To evaluate the demixing process under the non-isoquench depth condition, we carried out computer simulations of the time dependent concentration fluctuations using the Cahn–Hilliard non-linear diffusion equation. The simulations revealed that the SD under successive increases in quench depth yields the regular two-phase structure as in the case of the SD under isoquench, the structure coarsening is suppressed by the increase in quench depth, and the final morphology is highly dependent on the quench rate. The results adequately describe the characteristic features of structure development in the reaction-induced SD.

(Keywords: polymer blend; spinodal decomposition; computer simulation)

INTRODUCTION

Some dissimilar polymers with specific interactions are miscible at low temperatures and the mixtures phase separate at higher temperatures. This lower critical solution temperature (*LCST*) type of phase behaviour has been found for around 30 pairs of dissimilar polymers[1]. When the homogeneous mixture is allowed to undergo a rapid temperature jump from below the *LCST* to above the *LCST* and is annealed isothermally, the demixing takes place via a spinodal decomposition (SD). This yields a highly interconnected two-phase morphology with a unique periodicity. The isothermal SD is an interesting subject in the physics of ordering[2]. It is also interesting for the morphology design of polymer blends, since the characteristic morphology can be fixed or frozen by quenching the demixed system below the glass transition temperature (T_g) after an appropriate period of phase decomposition.

For materials design, more interesting is the SD induced by chemical reaction. This is typically illustrated by the polymerization of monomer A in the presence of polymer B. For example, polybutadiene (PB) is soluble in styrene monomer and the PB/styrene mixture is initially a single-phase system at the polymerization temperature (100°C); however, the system will be thrust into the two-phase regime as the polymerization proceeds to form polystyrene, and this elevates the upper critical solution temperature (*UCST*). Hence, the SD is expected to take place. High impact polystyrene (HIPS) and acrylonitrile–butadiene–styrene (ABS) resin are produced in this way. However, agitation is usually applied during the polymerization, so that it is very hard to analyse the SD process under a complicated shear field. In contrast, multicomponent thermoset resins such as epoxy/liquid rubber and epoxy/poly(ether sulfone) systems are prepared quiescently, which simplifies the situation. Light-scattering studies have revealed the SD nature of the reaction-induced phase separation in thermoset/thermoplastic systems[3–5]. Recently, a similar situation was also confirmed for the static polymerization of methyl methacrylate in the presence of poly(ethylene-*co*-vinyl acetate)[6]. In both cases, the regularly phase-separated structures in the fully cured or polymerized materials could be interpreted in terms of the structure formation mechanism via the SD.

The quiescent SD driven by reaction proceeds isothermally, but the quench depth, the temperature difference between the *LCST* (or *UCST*) and the reaction temperature, increases with time. The problem is then whether or not the SD really yields the regularly phase-separated structure in a manner similar to the SD under the isoquench depth. To investigate this problem is the objective of this paper. In this paper, we first give a brief review of the reaction-induced SD. Then, we present the results of computer simulations that use the Cahn–Hilliard non-linear diffusion equation for the time

* Present address: Central Research Laboratories, Kuraray, Sakazu, Kurashiki, Okayama 710, Japan
† On leave from the Department of Macromolecular Science, Fudan University, Shanghai 200433, China
‡ To whom correspondence should be addressed

0032-3861/94/17/3774–08

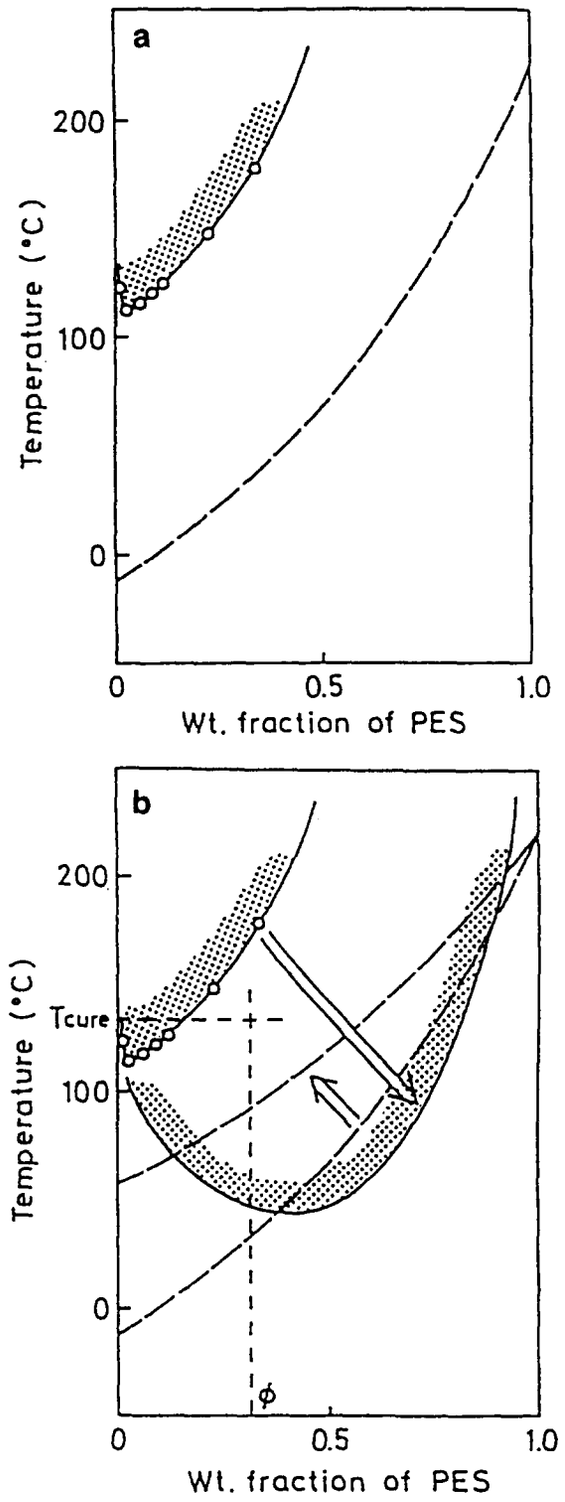

Figure 1 (a) Phase diagram of an epoxy ($M_n = 380$)/PES ($M_n = 17\,700$) mixture. (b) Schematic representation of the variations in the phase diagram and T_g (dashed line) with curing (reproduced from ref. 3)

dependent concentration fluctuations under successive increases in the quench depth. Finally, we compare the simulated results with the experimental results.

BACKGROUND: REACTION-INDUCED SPINODAL DECOMPOSITION

A binary mixture of poly(ether sulfone) (PES) and the diglycidyl ether of bisphenol A (epoxy) exhibits *LCST* phase behaviour[3]. On the basis of the current understanding of polymer/polymer miscibility, the *LCST* is expected to go down and the two-phase region should prevail in the phase diagram as the molecular weight of the epoxy increases with curing (chain extension). The T_g of the mixture should be elevated as the molecular weight increases. These situations are schematically illustrated in *Figure 1*. This figure implies that the mixture of composition ϕ is initially a single-phase system at T_{cure}; however, the system will be thrust into the two-phase regime as the curing reaction proceeds. *Figure 2a* shows the systematic change in the light-scattering profile with curing time when the epoxy/PES mixture is cured using 4,4′-diaminodiphenylmethane (DDM). This variation with time is characteristic of the SD, i.e. the scattering peak appears and the peak intensity increases, while its position shifts to smaller angles with time. This time dependence can be assigned to the coarsening process in the intermediate to late stages of the conventional thermally induced SD (under the isoquench depth). After 570 s, the scattering profile remains unchanged, suggesting morphology fixation. This is probably caused by vitrification on approaching the T_g or gelation in the epoxy-rich region. Scanning electron microscopy shows the formation of regularly interconnected spherical domains of epoxy in the PES matrix.

A binary mixture of the epoxy and amine-terminated butadiene/acrylonitrile liquid rubber (ATBN) exhibits *UCST*-type phase behaviour (*UCST* = −7°C)[4]. A low temperature cure (at room temperature) using a highly reactive curing agent, Versamid®, led to the time dependence of the light-scattering profile shown in *Figure 2b*. In this case, the scattering intensity increases with time but the peak angle of the scattering profile remains constant during the demixing. This implies that the coarsening to a longer interdomain spacing has been suppressed. By torsional braid analysis, the suppression was shown to occur before the gelation. This demixing behaviour is explicitly different from that of the familiar isoquench SD. Similar but slightly different results were obtained for the curing process of a binary mixture of epoxy and carboxy-terminated butadiene/acrylonitrile liquid rubber (CTBN) with a higher *UCST* (~65°C)[5] and the radical polymerization of a methyl methacrylate/poly(ethylene-*co*-vinyl acetate) mixture[6] (see *Figure 3*).

Another example is shown in *Figure 2c*, where an epoxy/CTBN mixture was cured using a curing agent with an extremely low reactivity (piperidine). The small-angle peak appeared after a certain time lag and its intensity increased at constant peak angle, then the wide-angle peak appeared at a fairly late stage just before the gel point[4]. The fully cured resin has a profile with two peaks. The small-angle peak can be assigned to the interdomain spacing between the large domains, while the wide-angle peak can be assigned to the overall spacing including small domains.

Thus, in the phase separations induced by chemical reaction, various time dependences in the light-scattering profile have been observed. As summarized in *Figure 3*, there are both similarities and differences with respect to the isoquench SD. However, in all cases the reaction-induced SD yields the regularly phase-separated morphology. As shown in *Figure 1b*, the phase separation proceeds isothermally under successive increases in the quench depth rather than under the isoquench depth. The problem is whether or not the reaction-induced SD really results in a regular two-phase system in a manner

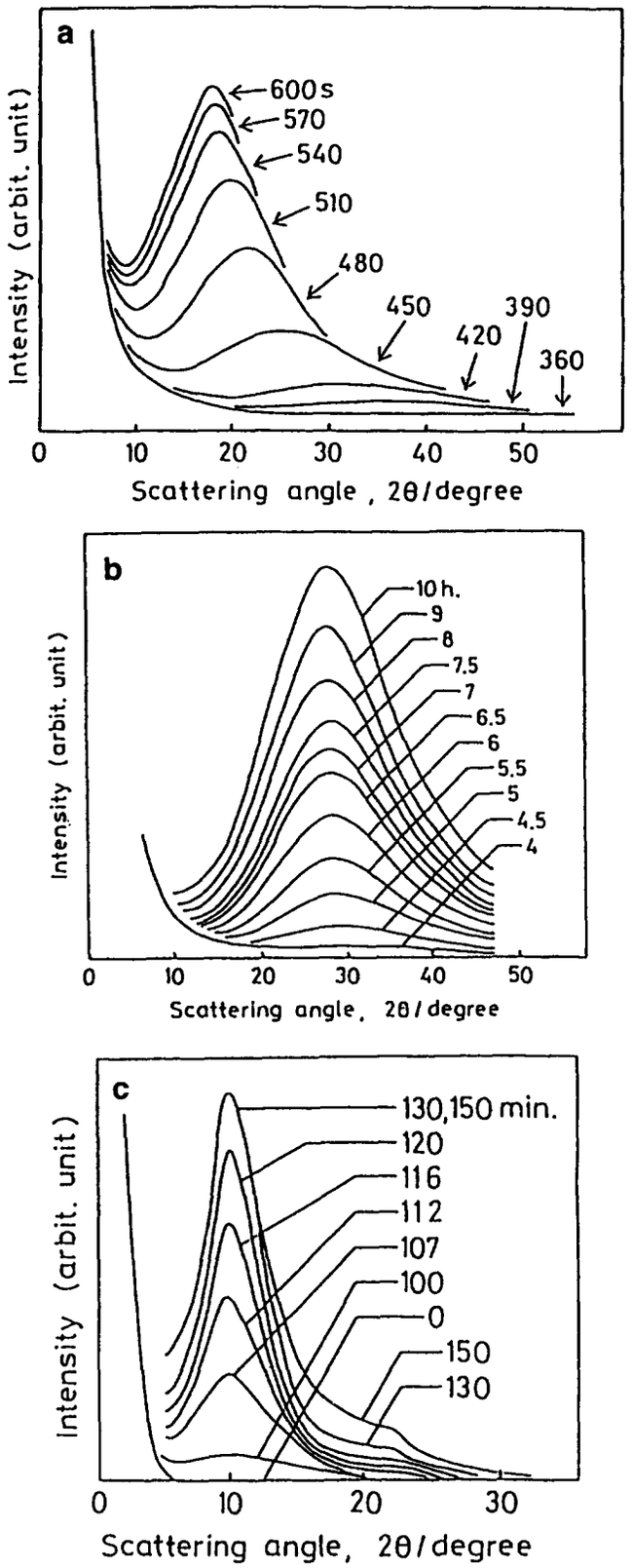

Figure 2 Changes in the light-scattering profile with curing for the following systems: (a) epoxy/PES/DDM (100/30/26; curing temperature = 140°C); (b) epoxy/ATBN/Versamid (100/45/50; curing temperature = 24°C); (c) epoxy/CTBN/piperidine (100/20/5; curing temperature = 90°C) [(a) is reproduced from ref. 3; (b) and (c) are from ref. 4]

similar to the decomposition under the familiar isoquench depth[8,9]. The problem is illustrated in *Figure 4*. Consider a two-step SD. Firstly, at a shallow quench the SD proceeds to give concentration profile A. What happens

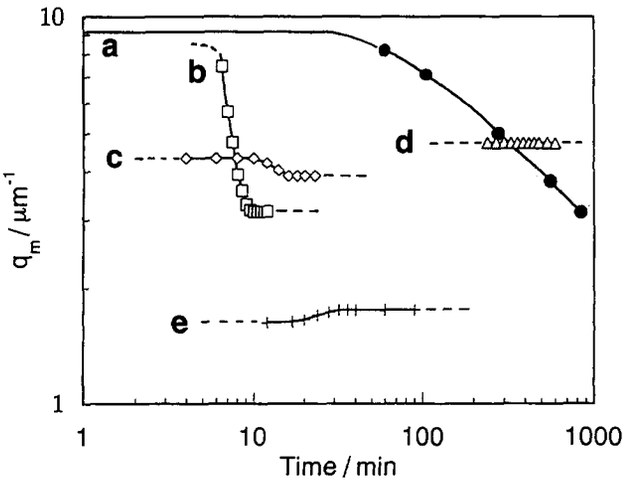

Figure 3 Time dependence of the scattering vector q_m with the maximum growth rate in the concentration fluctuation for the following systems: (a) polystyrene/poly(vinyl methyl ether) (isoquench, 101°C)[7]; (b) epoxy/PES/DDM[3]; (c) methyl methacrylate/poly(ethylene-*co*-vinyl acetate)/AIBN (90°C)[6]; (d) epoxy/ATBN/Versamid[4]; (e) epoxy/CTBN/DDM[5]

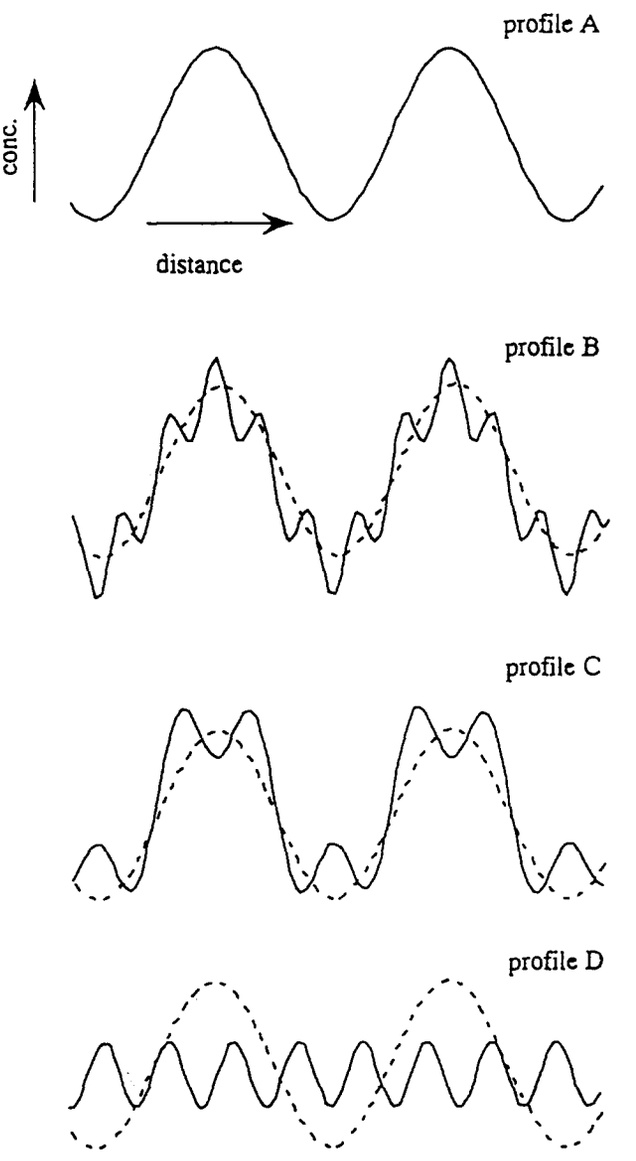

Figure 4 Schematic concentration profiles developed by the isothermal SD (profile A) and after a second jump to a deeper quench (profiles B–D)

when the system is thrust into a deeper quench? Three conceivable situations are shown: short waves expected at a deeper quench overlap with the long waves (profile B); short waves appear between long waves (profile C); and long waves degenerate while short waves develop (profile D). Furthermore, what happens at the third jump to a much deeper quench? Presently, we cannot provide an adequate answer to this complicated situation. In an attempt to clarify the situation, we carried out computer simulations of demixing with successive increases in the quench depth using the Cahn–Hilliard non-linear diffusion equation[10].

CALCULATION PROCEDURE

Diffusion equation

Mutual diffusion in a binary mixture with concentration fluctuations can be described by the non-linear diffusion equation presented by Cahn and Hilliard

$$\frac{\partial c}{\partial t}=\frac{\partial}{\partial x}\left(D\frac{\partial c}{\partial x}\right)-2M\kappa\left(\frac{\partial^4 c}{\partial x^4}\right) \tag{1}$$

where c is the concentration, x is the distance, t is the time, M is the mobility of the molecules and κ is the energy gradient coefficient. D is the diffusion coefficient defined by

$$D=M\left(\frac{\partial^2 f}{\partial c^2}\right) \tag{2}$$

where f is the local free energy of the mixture. For our numerical calculations, we express f in polynomial form

$$f(c)=a_n c^n+a_{n-1}c^{n-1}+\cdots+a_1 c+a_0 \tag{3}$$

D is also expressed in polynomial form as a function of the concentration fluctuation $q=c-c_a$

$$D(q)=D_m q^m+D_{m-1}q^{m-1}+\cdots+D_1 q+D_0 \tag{4}$$

where c_a is an average concentration. Since the relationship between D and f is given by equation (2), the D_i can be expressed as a function of the a_j (in the case of $n=6$)

$$D_0=30M[a_6c_a^4+(2/3)a_5c_a^3+(2/5)a_4c_a^2+(1/5)a_3c_a+(1/15)a_2] \tag{5a}$$

$$D_1=30M[4a_6c_a^3+2a_5c_a^2+(4/5)a_4c_a+(1/5)a_3] \tag{5b}$$

$$D_2=30M[6a_6c_a^2+2a_5c_a+(2/5)a_4] \tag{5c}$$

$$D_3=30M[4a_6c_a+(2/3)a_5] \tag{5d}$$

$$D_4=30Ma_6 \tag{5e}$$

In order to solve equation (1), the concentration fluctuation q must be expressed as a sum of Fourier series

$$q(x,t)=\Sigma Q_h \exp[2\pi xi/(L/h)] \tag{6}$$

where L is the longest wavelength of the Fourier component in the demixing system and Q_h is the amplitude of a Fourier wave with wavelength $L/|h|$ ($h=\pm1, \pm2,\ldots; h\neq0$). Then one obtains an equation describing the time dependence of the amplitude Q_h of every Fourier wave by inserting equations (4) and (6) into equation (1)

$$\frac{\partial Q_h}{\partial t}=-(hb)^2[(D_0+2h^2b^2M\kappa)Q_h+(1/2)D_1R_h+(1/3)D_2S_h+(1/4)D_3T_h+(1/5)D_4U_h] \tag{7}$$

where $b=2\pi/L$ and

$$R_h=\int_{-\infty}^{+\infty}Q_kQ_{h-k}\,dk$$

$$S_h=\int_{-\infty}^{+\infty}R_kQ_{h-k}\,dk$$

$$T_h=\int_{-\infty}^{+\infty}S_kQ_{h-k}\,dk$$

$$U_h=\int_{-\infty}^{+\infty}T_kQ_{h-k}\,dk$$

The time dependence of Q_h is calculated from

$$Q_h(t+\Delta t)=Q_h(t)+\left(\frac{\partial Q_h}{\partial t}\right)\Delta t \tag{8}$$

The concentration fluctuation at time t can therefore be obtained from equation (6).

Free energy function

For the free energy function f in our calculation, we employ the Flory–Huggins equation

$$f(c)=RTV[(c\ln c)/V_1+[(1-c)\ln(1-c)]/V_2+c(1-c)\chi/V_1] \tag{9}$$

where V_i is the molar volume of component i and χ is the interaction parameter between components. Following the equation of state theory, χ can be described by

$$\chi(T)=\frac{P_1^*V_1^*}{RT_1^*}\left[\frac{\tilde{V}_1^{1/3}}{\tilde{V}_1^{1/3}-1}\left(\frac{X_{12}}{P_1^*}\right)+\frac{\tilde{V}_1^{1/3}}{2(\frac{4}{3}-\tilde{V}_1^{1/3})}\tau^2\right] \tag{10a}$$

where

$$\tau=1-(T_1^*/T_2^*) \tag{10b}$$

$$\tilde{V}_i=V_i/V_i^* \tag{10c}$$

$$\tilde{V}_i^{1/3}=\alpha_iT/3(1+\alpha_iT)+1 \tag{10d}$$

and R is the gas constant. The starred parameters are the characteristic temperature (T_i^*), volume (V_i^*) and pressure (P_i^*). X_{12} is the exchange energy between segments of components and α_i is the thermal expansion coefficient. For the calculations, equation (9) must be expressed in polynomial form such as equation (3), because the concentration dependence of the free energy is introduced through the a_j in equation (3). As explained in the Appendix, equation (9) can be approximated in polynomial form using the least-squares method.

Successive quenches

In the calculation, a homogeneous binary mixture was first thrust into the two-phase region and allowed to demix isothermally for a while at a temperature T_0 (see *Figure 5*). After time t_0, the quench depth ΔT was then successively increased by $\beta\Delta t$, where β is the quench rate and Δt is the time increment which appears in equation (8). Since the free energy depends on temperature (see equations (9) and (10)), one must calculate the D_i for every quench depth in order to evaluate Q_h at that temperature. One can thus calculate the time dependence of the concentration fluctuations under successive increases in quench depth.

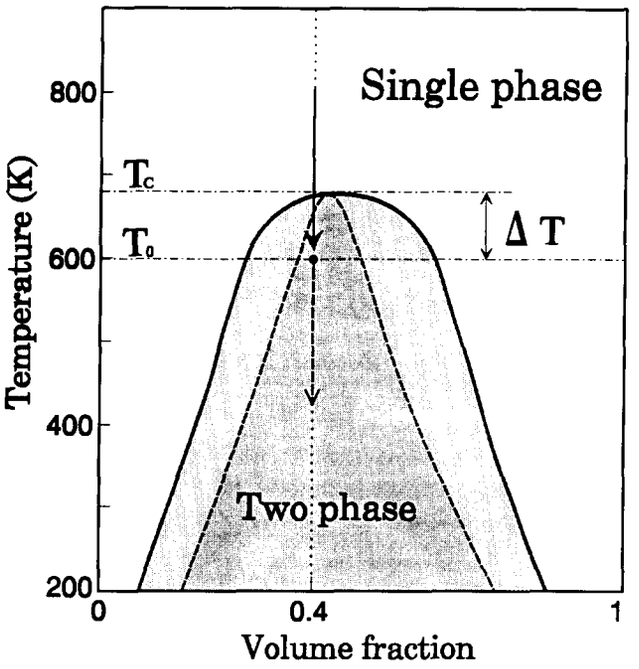

Figure 5 Phase diagram calculated with the equation of state parameters given in the text: (——) binodal; (– – –) spinodal

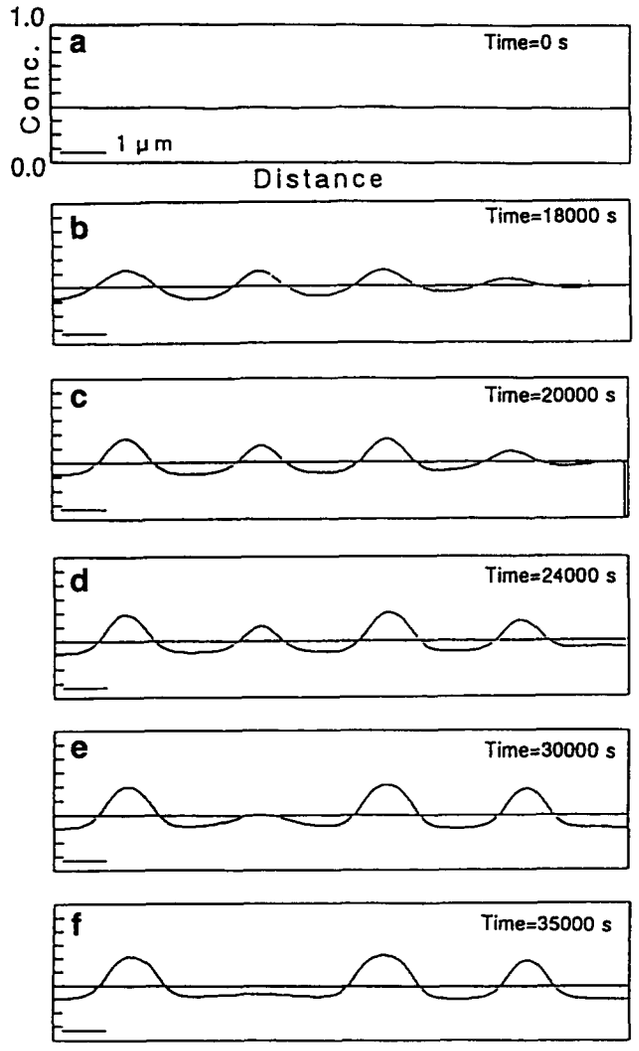

Figure 6 Time dependence of the concentration fluctuations during isothermal demixing at the two-phase region in *Figure 5*

Parameters

We used the equation of state parameters $V_1^* = 165\,000$ cm^3 mol^{-1}, $V_2^* = 100\,000$ cm^3 mol^{-1}, $T_1^* = 6571$ K, $T_2^* = 6715$ K, $P_1^* = 400$ J cm^{-3}, $X_{12} = 0.04$ J cm^{-3}, $\alpha_1 = 0.000685$ K^{-1} and $\alpha_2 = 0.000673$ K^{-1}. A phase diagram calculated with these parameters is shown in *Figure 5*. We also employed $c_a = 0.4$, $M = 1.55 \times 10^{-6}$ cm^2 s^{-1} and $\kappa = 3.50 \times 10^{-16}$ cm^2. For the numerical calculations, we used the maximum values $h = 256$, $L = 50\,\mu$m and $\Delta t = 0.1$ s.

RESULTS OF THE CALCULATIONS

Figure 6 shows the simulated results for the isothermal demixing behaviour of a 40/60 mixture at T_0 ($\Delta T = 80$ K) in *Figure 5*. We employ the Orstein–Zernike function to describe the concentration profile in *Figure 6a*, which corresponds to a concentration fluctuation just after the temperature jump from the single-phase region to the two-phase region. The fluctuation grows with a constant periodic distance during the early stages of demixing (*Figures 6a–6c*). The second peak in *Figure 6b* then starts to shrink and is finally absorbed into the neighbouring peaks. The structure coarsening thus proceeds under the evaporation/condensation mechanism and the average periodic distance increases with time (*Figures 6c–6f*).

The calculated results thus nicely describe the demixing behaviour characteristic to the SD, i.e. growth of the concentration fluctuation with a fixed periodic distance in the early stages and coarsening in the intermediate to late stages. In an earlier study, we compared the simulated

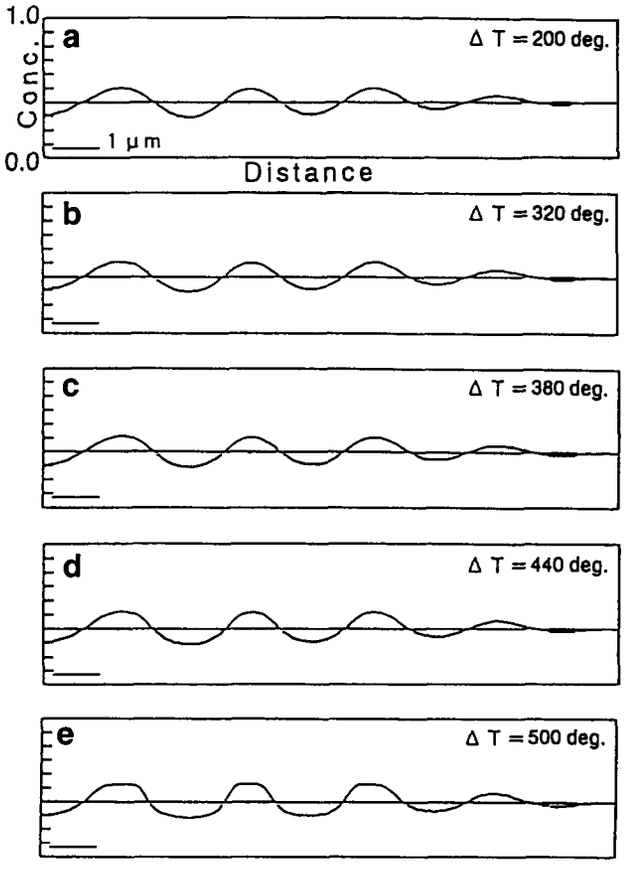

Figure 7 Time dependence of the concentration fluctuations during demixing with successive increases in the quench depth (quench rate = 6.0 K s^{-1})

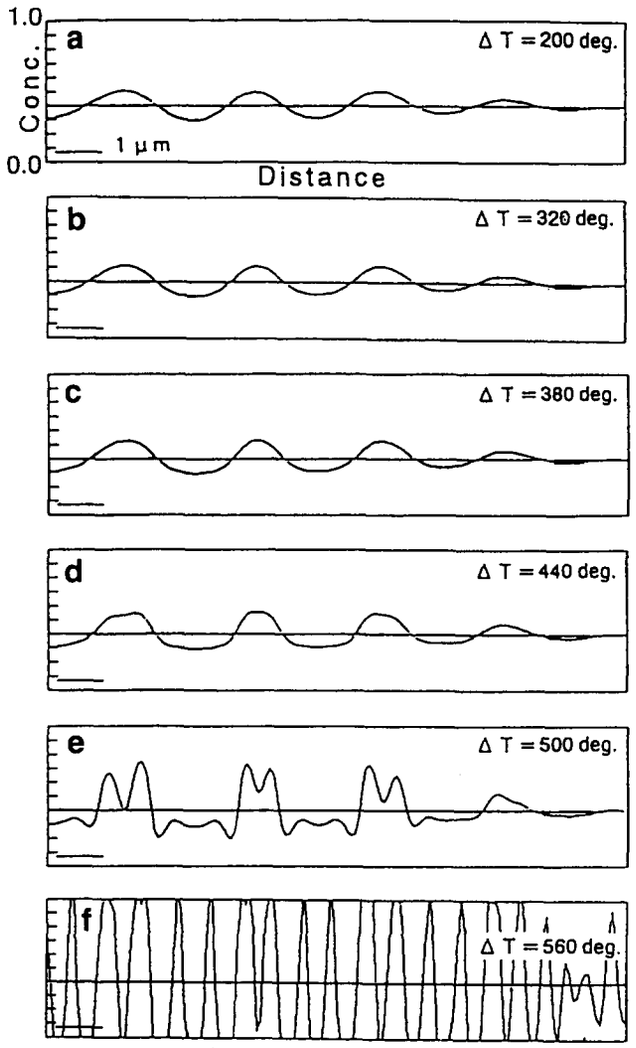

Figure 8 Time dependence of the concentration fluctuations during demixing with successive increases in the quench depth (quench rate = 3.0 K s^{-1})

and experimental time dependences for the wavelength of a dominant Fourier component in the concentration fluctuation, and confirmed the applicability of our simulation to polymer/polymer systems[10].

After the 40/60 mixture had been isothermally demixed at T_0 for 18 000 s ($t_0 = 18\,000$ s, $\Delta T = 80$ K), the quench depth was allowed to increase successively at a constant rate β. The value of the quench rate β was varied from 0.15 K s^{-1} to 6.0 K s^{-1}.

The results for the fast quench rate ($\beta = 6.0$ K s^{-1}) are shown in *Figure 7*. The initial concentration profile is preserved until the quench depth attains 440 K (*Figures 7a–7d*), and then the profile becomes rectangular (*Figure 7e*). The periodic distance and amplitude of the initial fluctuation are maintained even at the temperature of the deepest quench, i.e. the demixing barely proceeds throughout the successive quenches.

Figure 8 shows the results for a slower quench rate (3.0 K s^{-1}). The concentration profile becomes rather rectangular with successive quenches but the periodic distance remains constant (*Figures 8a–8d*). Then a rapid-growing concentration fluctuation with a shorter periodic distance appears and overlaps with the previous one (*Figure 8e*). The shorter periodic distance (*Figure 8f*) is about a quarter of the initial one (*Figure 6b*).

When the quench rate is reduced to 0.6 K s^{-1}, additional peaks appear between the original ones (*Figure 9c*). Both sets of peaks grow to establish a trapezoid/triangle alternating profile (*Figure 9e*). When the quench rate is further reduced to 0.3 K s^{-1}, the additional peaks again appear (*Figure 10b*), but they decay later (*Figures 10b–10d*) and eventually the trapezoidal profile remains (*Figure 10e*). At the slowest quench rate ($\beta = 0.15$ K s^{-1}), the additional peaks never appear and the profile just becomes rectangular and maintains its constant periodic distance (*Figure 11*).

DISCUSSION

The above results imply that the regular two-phase structure can be produced via phase separation with successive increases in the quench depth. However, the time dependence of the concentration fluctuations for the successive quenches was found to be different from that for the isoquench SD[8,9]. In the non-isoquench systems, the suppression of the coarsening was shown in various ways (*Figures 7–11*). This suggests that a change in the quench depth affects the demixing kinetics, and the simple scaling rules[11–16] will not be applicable for the non-isoquench systems.

In order to get a qualitative understanding of the coarsening suppression phenomenon, we should go back to equation (7). However, as we discussed in an earlier article[10], the linear term in the kinetic equation may be dominant, so we should first consider the demixing behaviour based on the linear term. The first term of

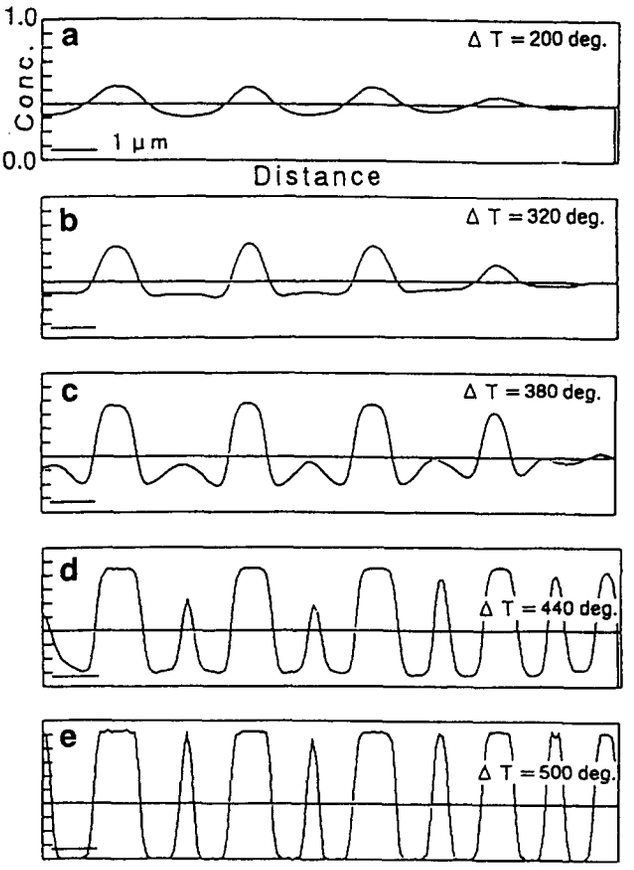

Figure 9 Time dependence of the concentration fluctuations during demixing with successive increases in the quench depth (quench rate = 0.6 K s^{-1})

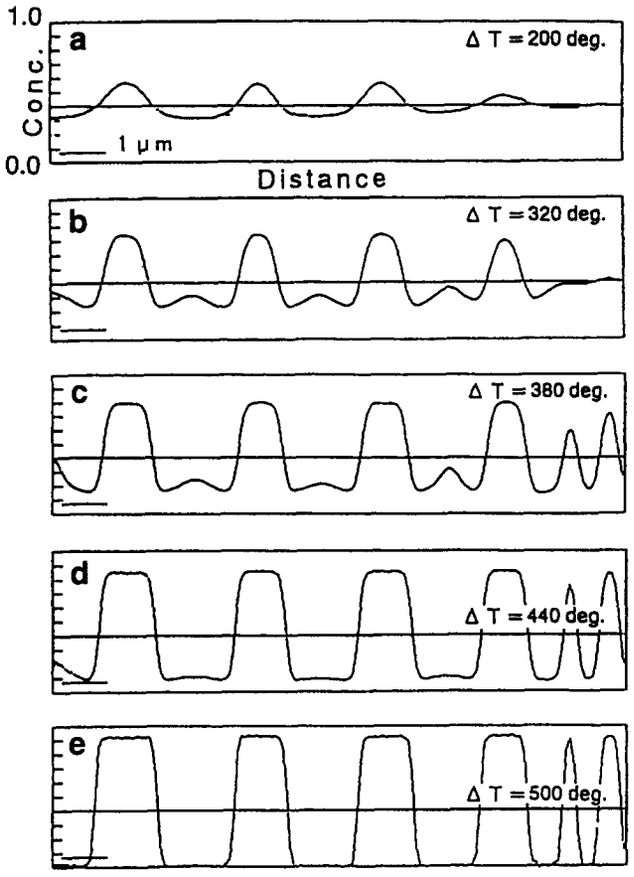

Figure 10 Time dependence of the concentration fluctuations during demixing with successive increases in the quench depth (quench rate = 0.3 K s^{-1})

equation (7) is the linear term, which is identical to the equation derived for the linearized theory of SD presented by Cahn[17]. In the context of Cahn's theory, the wavelength Λ_m of a dominant Fourier component in the concentration fluctuations is given by

$$\Lambda_m^2 = -16\pi^2\kappa/(\partial^2 f/\partial c^2) \qquad (11)$$

Since the absolute value of $\partial^2 f/\partial c^2$ becomes larger as the quench depth increases, Λ_m is expected to decrease with increasing quench depth for a fixed κ. The simulated results in *Figures 8–11* indicate that the periodic distance of the resulting two-phase structure in the later stages becomes shorter as the quench rate increases (except in the case where $\beta = 6.0\,K\,s^{-1}$). As clearly shown in *Figures 8* and *9*, a new fluctuation appears at a large quench depth. In the case where $\beta = 6.0\,K\,s^{-1}$ (*Figure 7*), the quench rate seems to be too high to yield a new fluctuation in the limited calculation time. In *Figures 10* and *11*, the new fluctuations appear and then decay. The decay may be caused by the non-linear terms, since one of their roles is to coarsen a two-phase structure. Thus, the non-linear terms may strongly affect the time dependence of the concentration fluctuations when the quench rate is slow. However, in these cases the linear term also plays an important role, so that a monotonic increase in the periodic distance of the concentration fluctuations is suppressed.

The situation in *Figure 7* seems to be realized in the epoxy/ATBN/Versamid system (*Figure 2b*), in which the chemical reaction proceeds quickly to give a large β. The results for the less reactive epoxy/CTBN/DDM system (*Figure 3e*) may correspond to the simulated results in *Figure 8*. The results for the low reactivity epoxy/CTBN/piperidine system (*Figure 2c*), which offers a light-scattering profile with two peaks, can be modelled by the simulated results in *Figure 9*. Actually, this system was shown to have a bimodal distribution of CTBN particles, as expected from the concentration profile in *Figure 9e*. Finally, the epoxy/PES/DDM system (*Figure 2a*) could be assigned to a system with a very small β. The time dependence of the light-scattering profile is very similar to that of the familiar isothermal SD, and the coarsening process is definitely seen. This situation could be simulated when β is set to less than 0.15 K s^{-1}. The low value of β means that the quench depth is not increased so dramatically as the molecular weight of the epoxy increases during the reaction. Actually, using the equation of state theory, Rostami recently predicted that the depression of the *LCST* with increasing molecular weight in the epoxy/PES system will be quite small[18].

CONCLUSIONS

Computer simulations using the Cahn–Hilliard non-linear diffusion equation were carried out to interpret the morphology formation during demixing driven by chemical reaction. The simulation results suggest that the monotonic increase in the periodic distance of the concentration fluctuation with time was suppressed by the successive increases in quench depth, and the growth mode of the concentration fluctuation changed with the

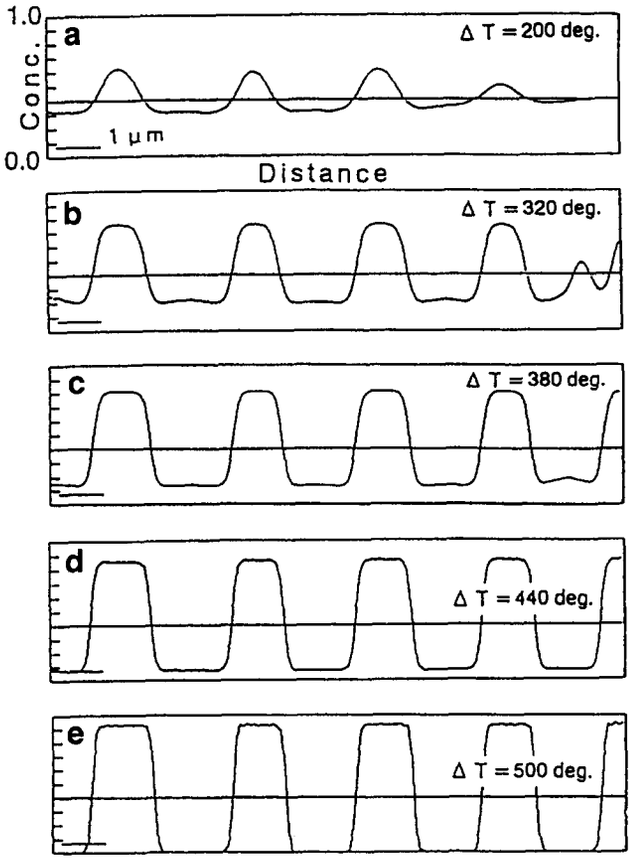

Figure 11 Time dependence of the concentration fluctuations during demixing with successive increases in the quench depth (quench rate = 0.15 K s^{-1})

quench rate. The time dependences of the concentration fluctuations observed in these simulations provide a nice explanation for the variety of morphologies formed by the reaction-induced SD.

REFERENCES

1 Olabishi, O., Robeson, L. M. and Shaw, M. T. 'Polymer–Polymer Miscibility', Academic Press, New York, 1979, Ch. 5
2 Komura, S. and Furukawa, H. (Eds) 'Dynamics of Ordering in Condensed Matter', Plenum Press, New York, 1988
3 Yamanaka, K. and Inoue, T. *Polymer* 1989, **30**, 662
4 Yamanaka, K., Takagi, Y. and Inoue, T. *Polymer* 1989, **60**, 1839
5 Yamanaka, K. and Inoue, T. *J. Mater. Sci.* 1990, **25**, 241
6 Kobayashi, S., Chen, W., Inoue, T., Ohnaga, T. and Ougizawa, T. *Macromolecules* in press
7 Hashimoto, T., Kumaki, J. and Kawai, H. *Macromolecules* 1983, **16**, 641
8 Hashimoto, T., Itakura, M. and Hasegawa, H. *J. Chem. Phys.* 1986, **85**, 6118
9 Bates, F. S. and Wiltzius, P. *J. Chem. Phys.* 1989, **91**, 3258
10 Ohnaga, T. and Inoue, T. *J. Polym. Sci., Polym. Phys. Edn* 1989, **27**, 1675
11 Hashimoto, T., Itakura, M. and Shimizu, N. *J. Chem. Phys.* 1986, **19**, 35
12 Takenaka, M., Izumitani, T. and Hashimoto, T. *J. Chem. Phys.* 1990, **92**, 4566
13 Takenaka, M., Izumitani, T. and Hashimoto, T. *J. Chem. Phys.* 1992, **97**, 6855
14 Song, M., Huang, Y., Cong, G., Liang, H. and Jiang, B. *Polymer* 1992, **33**, 1293
15 Kyu, T. and Lim, D. S. *Macromolecules* 1991, **24**, 3645
16 Maruta, J., Ohnaga, T. and Inoue, T. *Macromolecules* 1993, **26**, 6386
17 Cahn, J. W. *J. Chem. Phys.* 1965, **42**, 93
18 Rostami, S. personal communication, 1993

APPENDIX

In general, the logarithmic term $c \ln c$ in equation (9) can be approximated in polynomial form using the least-squares method

$$F(b_i)=\int_0^1 \left(c \ln c-\sum_{j=0}^{n} b_j c^j\right)^2 \mathrm{d}c \qquad \text{(A1)}$$

In equation (A1), we must choose b_i such that $F(b_i)$ takes a minimal value. By differentiating the equation, we obtain

$$\frac{\partial F}{\partial b_i}=-2\int_0^1 \left(c \ln c-\sum_{j=0}^{n} b_j c^j\right)c^i \,\mathrm{d}c \qquad \text{(A2)}$$

The b_i are obtained under the condition where the right-hand term of equation (A2) is zero. The condition is rewritten as follows

$$\sum_{j=0}^{n} b_j \int_0^1 c^i c^j \,\mathrm{d}c=\int_0^1 (c \ln c)c^i \,\mathrm{d}c \qquad \text{(A3)}$$

Equation (A3) can be integrated to give

$$\sum_{j=0}^{n} b_j/(i+j+1)=-1/(i+2)^2 \qquad \text{(A4)}$$

By solving equation (A4) ($n=6$, $i=0$–6 in this calculation), we can obtain the b_i and express $c \ln c$ in polynomial form. The logarithmic term $(1-c)\ln(1-c)$ in equation (9) can also be processed using the method described above, and therefore equation (9) can be given in polynomial form and the a_j in equation (3) are expressed as follows

$$a_6=b_6/V_1+b_6/V_2 \qquad \text{(A5a)}$$

$$a_5=b_5/V_1-(6b_6+b_5)/V_2 \qquad \text{(A5b)}$$

$$a_4=b_4/V_1+(15b_6+5b_5+b_4)/V_2 \qquad \text{(A5c)}$$

$$a_3=b_3/V_1-(20b_6+10b_5+4b_4+b_3)/V_2 \qquad \text{(A5d)}$$

$$a_2=b_2/V_1+(15b_6+10b_5+6b_4+3b_3+b_2)/V_2-\chi/V_2 \qquad \text{(A5e)}$$

$$a_1=b_1/V_1-(6b_6+5b_5+4b_4+3b_3+2b_2+b_1)/V_2+\chi/V_2 \qquad \text{(A5f)}$$

$$a_0=b_0/V_1+(b_6+b_5+b_4+b_3+b_2+b_1+b_0)/V_2 \qquad \text{(A5g)}$$